Dicyanopolyynes: A Homologuous Series of End-Capped Linear sp Carbon

Günther Schermann, Thomas Grösser, Frank Hampel, and Andreas Hirsch*

Abstract: The synthesis, isolation, spectroscopic characterization, and computational investigations of the rod-shaped dicyanopolyynes **1**–**6** ($C_{2n}N_2$, $n = 4$–9), which are model substances for the hypothetical one-dimensional carbon allotrope carbyne sp-C_∞, are described. Based on the trends in the spectroscopic behavior of **1**–**6** with increasing chain length, the electronic as well as the NMR properties of carbyne are predicted. For the investigation of the synthetic potential of this compound class, a first selected series of regioselective derivatizations is presented with the synthesis of the [4+2] and [3+2] cycloadducts **7**–**12**.

Keywords
ab initio calculations · alkynes · carbon allotropes · electronic structure · semiempirical calculations

Introduction

We reported recently on the first synthesis and identification of the dicyanopolyynes **1**–**5** ($C_{2n}N_2$, $n = 4$–8) as well as on the isolation and complete spectroscopic characterization of the smallest member of this family C_8N_2 (**1**).[1] Together with the already known representatives of this compound class—NC-CN, NC-C≡C-CN, and NC-C≡C-C≡C-CN[2]—**1**–**5** form a continuous homologous series of neutral rod-shaped molecules that possess the highest possible number of π electrons. They are isoelectronic with the all-carbon rods $(C{\equiv}C)_n^{2-}$ and, in analogy to the polyynes R-(C≡C)$_n$-R where R is a bulky alkyl-, silyl-, or aryl group,[3–7] or a transition metal complex fragment,[8] they can be considered as end-capped model substances for the hypothetical one-dimensional carbon allotrope carbyne sp-C_∞.[3] Polyynes similar to **1**–**5** such as HC_nN ($n = 1, 3, 5, 7$) have been detected by Kroto et al. as molecules in interstellar space.[9] In this comprehensive study we report for the first time on the isolation and spectroscopic characterization of the new homologues **1**–**5** and of the next homologue, the 20-atom rod $C_{18}N_2$ (**6**), which we obtained following the same workup procedure. In addition, we present computational investigations on the geometries and electronic structures of **1**–**6**, which explain the observed spectroscopic behavior. By extrapolating the characteristic trends in the spectroscopic data of **1**–**6** with increasing chain length, we predict properties of carbyne sp-C_∞. For the investigation of the synthetic potential of this compound class, we present a first selected series of regioselective derivatizations by allowing **1** and **2** to undergo [4+2] and [3+2] cycloaddition reactions with dienes and 1,3-dipoles.

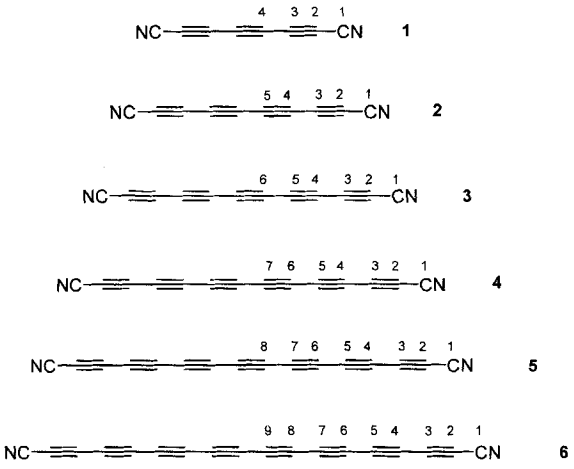

Results and Discussion

The synthesis of the dicyanopolyynes **1**–**6** was achieved by vaporization of graphite under Krätschmer–Huffman conditions[10] in the presence of cyanogen $(CN)_2$[11] as described earlier.[1] This very convenient method allows facile access to gram quantities of the new rod-shaped molecules **1**–**6** in one reaction step and avoids successive acetylene coupling, protection, and activation sequences involving unstable intermediates, which would be required for a conventional synthesis. Presumably, instead of efficiently condensing to fullerenes or heterofullerenes, growing carbon clusters[12–23] within the plasma are trapped by radicals such as ·CN to form the rod-shaped molecules **1**–**6**, while the generation of fullerenes is completely suppressed.[1] Temperatures of up to 6000 °C in the hot reaction zone of the arc vaporizer are responsible for the formation of radical cleavage products of cyanogen. The use of chlorine instead of cyanogen as added gas leads to the formation of

[*] Prof. Dr. A. Hirsch, Dipl.-Chem. G. Schermann, Dr. T. Grösser, Dr. F. Hampel
Institut für Organische Chemie, Henkestr. 42, 91054 Erlangen (Germany)
e-mail: hirsch@organik.uni-erlangen.de

  0947-6539/97/0307-1105 $ 17.50+.50/0

perchlorinated aromatics such as hexachlorobenzene or octachloroacenaphtylene, whose carbon skeletons represent sections of the C_{60} structure.[1]

The dicyanopolyynes **1**–**6** were the major soluble products formed during the graphite vaporization. They were separated from the soot by extraction with toluene and filtration to give a lemon-yellow solution. When chromatographed on silica gel (toluene/hexane 80:20) the polyynes **1**–**6** eluted together as the least polar fraction. More polar components were not identified. The mixture of **1**–**6** was obtained in 7% yield with respect to evaporated graphite and consisted of 55% **1**, 35% **2**, and 10% **3**–**6**. The isolation of **1**–**6** was achieved by preparative HPLC on an RP-18 phase with acetonitrile as eluent. The smallest polyyne **1** could be separated from the higher homologues with a purity of 98.9% (GC) and also by sublimation at room temperature at a pressure of 1 mbar.

The polyynes **1**–**6** form colorless crystals, which are very soluble, for example, in chloroform and toluene, but only sparingly soluble in hexane. In the solid state they are only stable at low temperatures in the dark. At room temperature slow decomposition takes place leading to black insoluble presumably cross-linked polymers. This decomposition occurs explosively if the crystals are exposed to shock or heat. Dilute solutions are indefinitely stable at −18 °C in the dark. The stability in solution at room temperature and in daylight, however, is sufficient to allow chromatographic separation and spectroscopic characterization. The stability of the polyynes decreases with increasing chain length. For example, concentrated solutions of **1** are stable at room temperature, whereas those of **6** slowly decompose, turning amber and finally forming a black insoluble precipitate. Similar trends have been reported for polyynes end-capped with bulky organic or organometallic groups.[4–8] The dicyanopolyynes **1**–**6** are less stable than those containing bulky end groups, since, for example, a C_{20} rod end-capped with sterically demanding Re-complex fragments is stable in the solid state at room temperature,[8] whereas solid $C_{18}N_2$ decomposes under these conditions. Bulky end groups keep the carbon chains in the crystal further apart from each other and thus prevent facile polymerization. These polymerizations may be similar to the topochemically controlled polymerizations of diacetylenes to polydiacetylene through a sequence of 1,4-additions investigated by Wegner.[24] With these studies, it was elegantly demonstrated that the distance between the chains is a critical factor for bringing about the polymerization process. It is to be expected that the shortest possible interchain distances (van der Waals contacts) can easily be achieved in crystals or concentrated solution of **1**–**6**, since no bulky end groups are present. Hence, with respect to their stability in the solid state, **1**–**6** are good short-chain model substances for carbyne sp-C_∞, which is expected to be extremely unstable.[3–9] It is therefore very questionable whether the material obtained by Lagow et al.[25] is the sp-carbon allotrope. The authors vaporized graphite in the presence of cyanogen using a similar procedure to that which we described earlier[1] and claim, without providing convincing experimental evidence, that chains with more than 300 (!) sp-C atoms are thermally stable even in the solid state. In our hands **6** is the largest isolable chain and, as mentioned above, it is already an unstable compound, which requires careful handling.

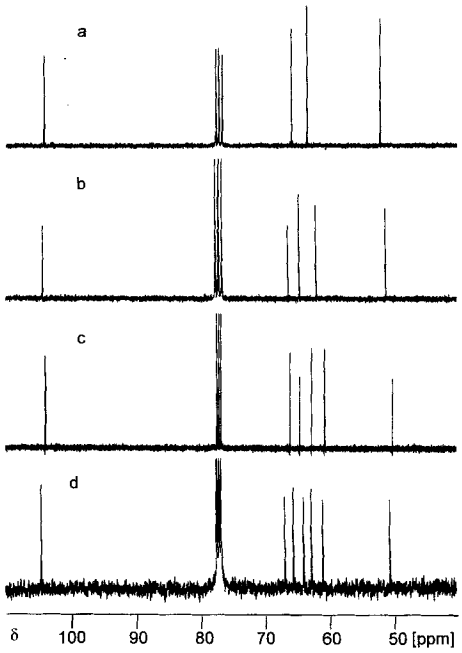

Figure 1. ^{13}C NMR spectra (62.9 MHz, 25 °C, $CDCl_3$) of a) C_8N_2 (**1**), b) $C_{10}N_2$ (**2**), c) $C_{12}N_2$ (**3**) and d) $C_{14}N_2$ (**4**).

The ^{13}C NMR spectra of the polyynes **1**–**4**[26] (Figure 1) are very characteristic and unambiguously allow the structure determination of these rod-shaped molecules. The cyano groups of the dicyanopolyynes appear at $\delta = 104$, and the alkyne C atoms in the expected region between $\delta = 50$ and 67. The chemical shifts of the cyano C atoms at $\delta = 104$ as well as those of the neighboring alkyne C-2 atoms at $\delta = 50$ are almost independent of the chain length and are very close to the corresponding values for C atoms[2] in cyanoacetylene ($\delta = 104.5$, 57.4), dicyanoacetylene ($\delta = 103.3$, 55.2), and dicyanodiacetylene ($\delta = 103.9$, 53.4). The high-field shift of the signals due to the C-2 atoms is caused by the cyano groups. A new signal appears in the narrow region between $\delta = 60$ and 67 with each chain extension by a C_2 unit, and the the signals in this region are almost always equidistant. The assignment of these and further signals was facilitated by the comparison of the experimental spectra with those obtained from the program SpecInfo,[27] which predicts a) signals for the cyano groups of each polyyne at $\delta = 104.85$, b) signals for the C-2 atoms at highest field at $\delta = 56.40$, c) signals for C-3 at lowest field at $\delta = 66.00$, d) signals for C-4 at second highest field at $\delta = 60.57$, and e) signals for all the remaining inner C atoms at $\delta = 61.95$. Comparison of the ^{13}C NMR data of **1**–**4** with those available for other polyynes (examples synthesized by Diederich[7] and Gladysz[8]) reveals an interesting conformity: Except for the signals of the sp-C atoms in direct or close proximity of the end groups like C-2 in **1**–**4** or C-2 and C-3 in the Re*-capped polyynes,[8] the signals of the inner sp-C atoms appear in the narrow region between $\delta = 60$ and 67. Hence, it is to be expected that the ^{13}C NMR spectra of polyynes R-$(C{\equiv}C)_n$-R with n approaching infinity will contain one broad signal at $\delta \approx 63$.

The FT-IR spectra were recorded for films on NaCl plates obtained by carefully allowing droplets of chloroform solutions of the polyynes **1**–**6** to evaporate. The spectra reveal only very

0947-6539/97/0307-1106 $ 17.50+.50/0 Chem. Eur. J. 1997, 3, No. 7

few vibrational modes and are dominated by the CN valence mode at $\tilde{\nu} = 2240\ cm^{-1}$. The valence modes of the CC triple bonds are weaker and appear between $\tilde{\nu} = 2090$ and $2120\ cm^{-1}$. In the FD mass spectra of **1**–**6**, the signals due to the M^+ ions appear as the only peaks, and no fragmentation is observed.

The electronic absorption spectra of **1**–**6** are of special interest. They can accurately be interpreted with the calculated MO diagrams and are in qualitative agreement with the spectra predicted by the ZINDO/S method.[28] The electronic absorption properties of the polyynes **1**–**6** also provide a beautiful example for the classical description of a one-dimensional electron gas, taking into account a periodic potential along the carbon chain due to bond length alternation.[29] There is at least one set of distinct bands with vibrational fine-structure in the UV region of each spectrum (Figure 2).

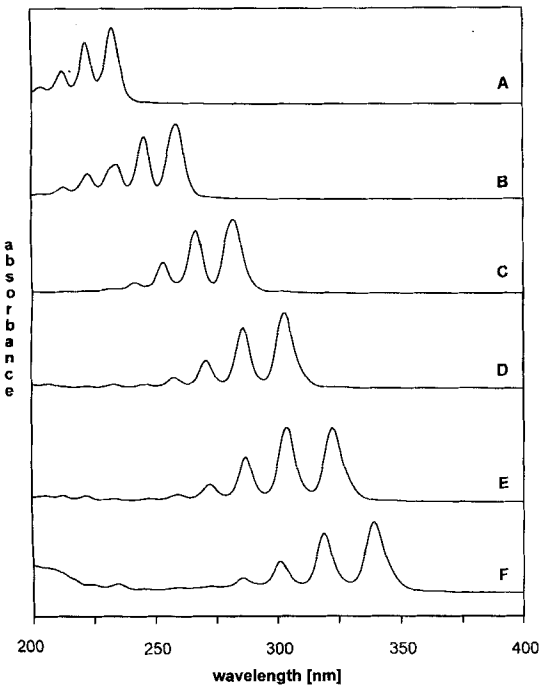

Figure 2. UV/Vis spectra (acetronitrile, 25 °C) of A) C_8N_2 (**1**), B) $C_{10}N_2$ (**2**), C) $C_{12}N_2$ (**3**) D) $C_{14}N_2$ (**4**), E) $C_{16}N_2$ (**5**) and F) $C_{18}N_2$ (**6**).

The longest-wavelength absorptions are in general the most intense in each spectrum. The positions of the absorptions strongly depend of the chain length of the dicyanopolyynes **1**–**6**. With increasing n and hence with the increasing length of the conjugated π-electron system, the absorption bands successively shift to longer wavelengths. The extent of the bathochromic shift increases with decreasing n. The same behavior has been observed by Bohlmann[4, 5] and Walton[6] for a series of polyynes containing bulky terminal groups. The sets of fine-structured absorptions of **1**–**6** shown in Figure 2 can be correlated by means of the empirical Lewis–Calvin equation[30] commonly written as $\lambda^2 = kn$ (λ = wavelength of corresponding bands for polyynes containing n conjugated triple bonds). This equation was originally formulated and applied to polyenes and was later used also by Walton et al.[6] to describe the absorption behavior of compounds R-$(C{\equiv}C)_n$-R, where R is H, silyl, alkyl, or aryl. For the series **1**–**6**, the plot of n versus the highest observed wavelength (λ^2) is a good straight line with slope of $k = 12.2 \times 10^3\ nm^2$ per triple bond (Figure 3), which is a typical value for polyynes. For the high-intensity bands, the average vibrational spacing $\Delta\lambda$ of corresponding adjacent bands in each polyyne increases with increasing chain length. The plot of $\Delta\lambda$ versus n also shows linear behavior and reveals a good correlation with the empirical relationship $\Delta\lambda = k'n$.

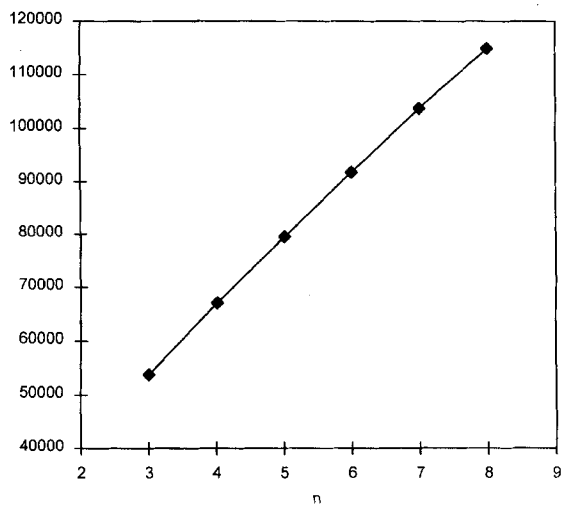

Figure 3. Lewis–Calvin plot ($\lambda^2 = kn$) for dicyanopolyynes **1**–**6**.

The observed spectroscopic behavior correlates well with the decrease in the HOMO–LUMO gaps with increasing chain length. The MO diagrams and hence the HOMO–LUMO differences were calculated at the MP2/3-21G* and HF/3-21G* levels of theory as well as semiempirically by the AM1 method implemented with the program package SPARTAN 4.0[31] (Figure 4, Table 1). The HOMOs are successively raised in energy,

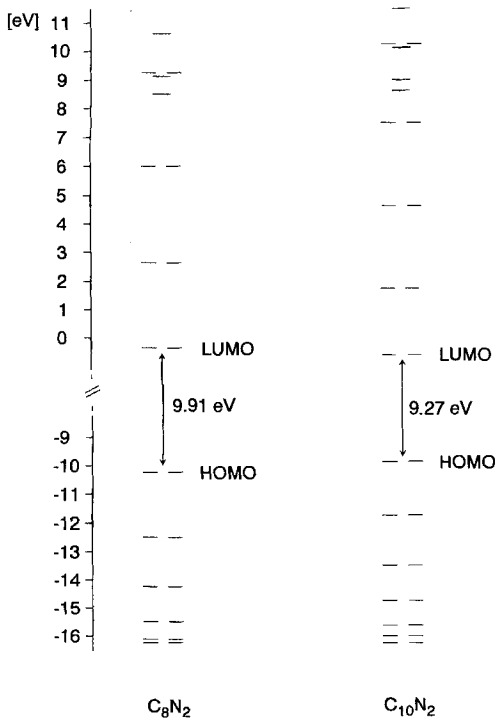

Figure 4. MO diagrams (MP2/3-21G*) for C_8N_2 (**1**) and $C_{10}N_2$ (**2**).

  0947-6539/97/0307-1107 $ 17.50+.50/0

Table 1. Lowest-energy absorptions in the UV/Vis spectra of **1**–**6**, calculated energy differences between HOMOs and LUMOs, and calculated transitions with oscillator strengths.

Polyyne	λ_{max} [a] [nm]	ΔE [b] [eV]	ΔE [c] [eV]	λ_{max} [d] [nm]	Os [e]	λ_{max} [f] [nm]	Os [e]
C_8N_2 (**1**)	232	10.79	9.01	186	6.36	119	1.71
$C_{10}N_2$ (**2**)	259	10.20	8.60	204	7.30	131	1.86
$C_{12}N_2$ (**3**)	282	9.79	8.23	220	8.14	143	2.00
$C_{14}N_2$ (**4**)	303	9.49	8.06	233	8.90	153	2.10
$C_{16}N_2$ (**5**)	322	9.28	7.90	244	9.62	163	2.18
$C_{18}N_2$ (**6**)	339	9.09	7.79	253	10.29	171	2.32

[a] Experimental value of the lowest energy absorption. [b] ΔE(HOMO–LUMO) calculated at HF/3-21G*. [c] ΔE(HOMO–LUMO) calculated by AM1. [d] ZINDO/S-calculated UV-spectrum (lowest-energy absorption). [e] Oscillator strength. [f] ZINDO/S-calculated next-higher symmetry-allowed transition.

whereas the LUMO energies are lowered. In analogy to the experimentally observed bathochromic shifts, the extent of narrowing of the HOMO–LUMO gaps decreases with increasing n. Owing to their $D_{\infty h}$ symmetry, the MOs in the frontier orbital region are doubly degenerate and exhibit alternately e_g and e_u symmetry. The HOMOs for polyynes with an even n have e_g symmetry and those with an odd n e_u symmetry. The HOMO–LUMO transitions are always symmetry allowed, whereas the HOMO–LUMO+1 transitions are symmetry forbidden. AM1 as well as MP2/3-21G* and HF/3-21G* calculations overestimate the HOMO–LUMO gaps (Table 1).

The same trend is also reflected by the ZINDO/S-calculated UV spectra. The λ_{max} values of the longest-wavelength absorptions of the calculated spectra are smaller than the experimental values by a factor of about 0.8. However, the bathochromic shift of the λ_{max} values with increasing n is in complete agreement with experiment, especially since the Lewis–Calvin plots of the calculated spectra also show linear behavior. The MO calculations show that the pattern of intense absorption bands are due to the vibrational fine-structure rather than to transitions into higher excited states. Symmetry-allowed transitions into excited states (HOMO → LUMO+2n) would occur at much higher energies and would be much less intense, since, for example, the oscillator strength of the second allowed transition is about a quarter of that of the first transition (Table 1). In the short-wavelength region of the UV/Vis spectra of **5** and **6** (Figure 2), a second set of less intense absorptions are indeed observed (between 200 and 240 nm). In the light of the theoretical calculations, these can be assigned to the next-higher symmetry-allowed transitions (HOMO → LUMO+2). Here the intensity ratios of the corresponding bands are in good agreement with the calculated oscillator strengths. For example, the ratio of the oscillator strengths of the second and first symmetry-allowed transition in **6** is calculated to be 0.23; the experimental ratio of intensities for the bands at λ_{max} = 234 and 339 nm is 0.18. The vibrational fine-structure of the UV bands of **1**–**6**, with the lowest-energy absorptions being the most intense, clearly shows that the Morse function of the first excited state is almost only vertically shifted with respect to the ground state. The oscillator strength of a given transition increases with increasing chain length. The experimental verification of the latter prediction is hampered because the dicyanopolyynes **1**–**6**, especially the higher homologues, are too unstable in the solid state to allow accurate weighing for the determination of the extinction coefficients. However, increasing intensity of absorption bands with increasing chain length has been observed for more stable polyynes investigated, for example, by Walton and Gladysz.[6, 8]

Analysis of the MP2/3-21G*-calculated structures of **1**–**6** shows that bond-length alternation between triple and single bonds decreases from the ends of the rods to the middle (Figure 5). A similar picture emerges for the bond orders: the single

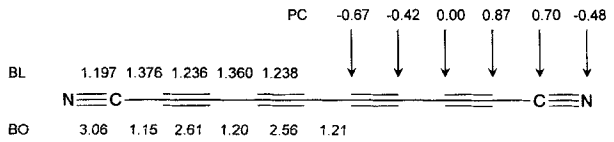

Figure 5. MP2/3-21G* bond lengths (BL), bond orders (BO), and partial charges in $C_{10}N_2$ (**2**).

and triple bonds increasingly gain double-bond character towards the middle. Hence, the molecules exhibit some cummulene character at their center, and this trend increases with increasing chain length.

For infinite chains two scenarios can be considered:

1) For large n there will be no bond length alternation in the interior of the chain.
2) The bond length equalization will never be complete, and the differences in length between "single" and "triple" bonds will approach a given limit.

In the former case $C_\infty N_2$ would be a black metal-like material, since the energy difference between HOMOs and LUMOs or the valence and conduction bands would disappear.[32] In the latter case $C_\infty N_2$ would be an insulator with an energy gap ΔE between valence and conduction bands.[32] The magnitude of ΔE and hence the color of $C_\infty N_2$ would then depend on the extent of the remaining bond length alternation.[29, 32] The same considerations are in principle also valid for C_∞ chains with terminal groups other than CN, including carbyne. Based on the present knowledge of the structures and electronic properties of one-dimensional solids, it is likely that bond length alternation in infinite sp carbon chains persists, termed Peierls distortion in solid state physics.[32] This distortion, which is related to the Jahn–Teller distortion in molecular chemistry, leads to a stabilization of the occupied MOs and to a destabilization of the unoccupied MOs, and stabilization or destabilization increases towards the frontier orbitals. Peierls distortion is a well-known phenomenon in the polyenes $(CH{=}CH)_n$.[32] Consequently, polyacetylene in the undoped state is an insulator with a lowest-energy absorption of λ_{max} = 650 nm.[33] This value is close to the estimated λ_{max} of 680 nm for $(CH{=}CH)_\infty$ obtained form the experimental absorption spectra of discrete polyene oligomers with various chain lengths by extrapolating the plot of E_{exp} versus $1/n$ to $n = \infty$ (E_{exp} = experimental optical absorption energy).[33] Whereas the spectroscopic behavior of short-chain representatives of polyenes[33] and polyynes (vide supra) can be described with the Lewis–Calvin equation $\lambda^2 = kn$, a better description for the long-chain analogues is provided by the empirical equation $E = a + b/n$,[33] since for larger n the plots E_{exp} versus $1/n$ become linear and approach a limiting value of $a \neq 0$ for $n \to \infty$ (Figure 6). Hence, by analogy to the polyenes, it can be predicted that bond length alternation between "single" and

0947-6539/97/0307-1108 $ 17.50+.50/0 Chem. Eur. J. 1997, 3, No. 7

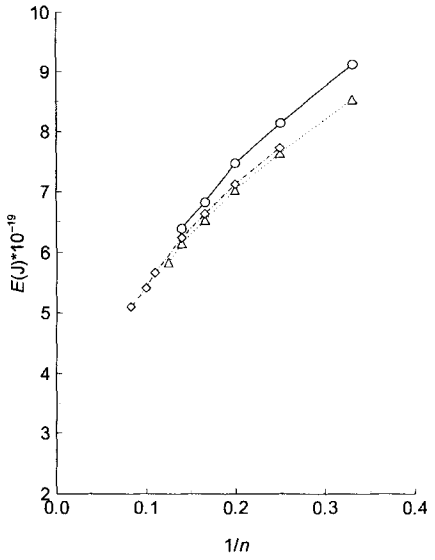

Figure 6. Lowest-energy absorption E [J × 10^{-19}] versus $1/n$ of R-$(C{\equiv}C)_n$-R. △: R = CN, ○: R = *t*Bu,[4] ◇: R = Et_3Si.[6a]

"triple" bonds also persists in polyynes and reaches a lower limit for infinite chain lengths. Based on the plot E_{exp} versus $1/n$ of the absorption data of **1**–**6**, λ_{max} of $C_\infty N_2$ is estimated to approach 550 nm for $n \rightarrow \infty$. Significantly, the corresponding plots for the series R-$(C{\equiv}C)_\infty$-R (R = *t*Bu, Et_3Si)[4, 6a] also become linear with increasing chain length and approach the same value (Figure 6). The differences in the plots for the shorter chains are due to the different end groups (end group effect). These effects become unimportant for very long chain lengths. Based on these considerations carbyne should be a colored insulating material.

The highest positive Mulliken partial charges on the $(C{\equiv}C)_n$ chains of **1**–**6** are located at C-2, followed by the C-3 position (Figure 5). The polarizations of the C-2/C-3 triple bonds are significantly larger than for all the other triple bonds in the middle of the chains. This charge distribution in the carbon chains induced by the cyano groups is the governing factor determining the regiochemistry of cycloadditions, as will be shown for a series of [4+2] and [3+2] cycloadditions carried out with the polyynes **1** and **2**. These were treated with 9,10-dimethylanthracene or 2,3-dimethylbutadiene in toluene, and the reaction mixtures were purified by column chromatography. Compounds **7**–**9**, formed by [4+2] cycloaddition at the first C–C triple bonds between C-2 and C-3, were obtained as the only monoaddition products. The completely characterized compounds **7**–**9** form bright yellow crystalline solids, which are totally stable under ambient conditions. Above 150 °C they decompose without melting. Whereas the monoadducts **7**–**9** were the major reaction products with one equivalent of the diene, [4+2] bisadducts **10** and **11** formed preferentially with an excess of diene. These successive additions to the terminal C–C triple bonds of **1** and **2** are regioselective processes, since the symmetrical bisadducts **10** and **11** are the only regioisomers that were found in the reaction mixtures. The higher symmetry of **10** and **11**, leading to favorable packing in the crystal, presumably explains why they are much less soluble than the monoadducts **7** and **8**. Single crystals of **10** suitable for X-ray analysis were obtained by allowing cyclohexane solutions to evaporate slowly

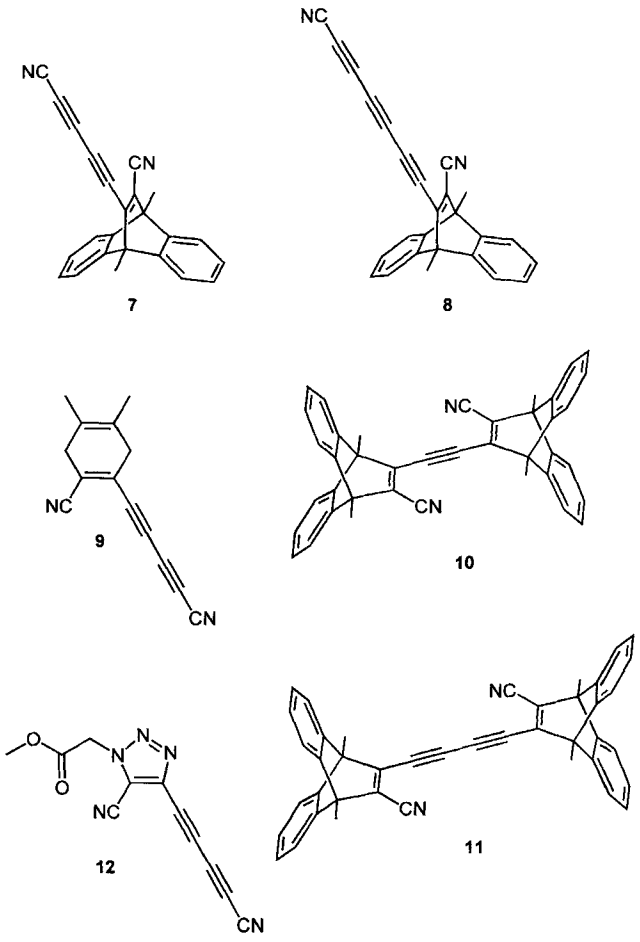

(Figure 7). In the crystal **10** has C_{2h} symmetry. The dicyano–diene–yne chain is planar, which guarantees the most favorable orbital overlap within the conjugated π-electron system.

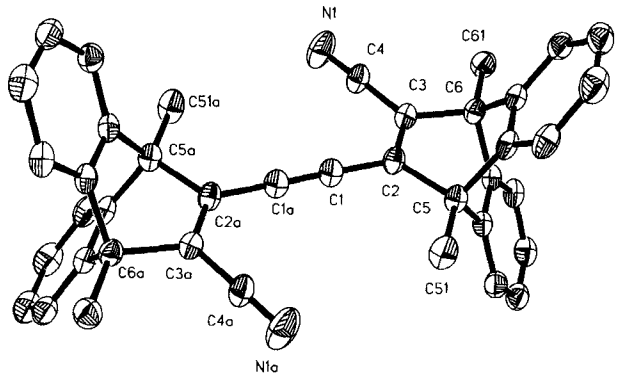

Figure 7. X-ray crystal structure of **10**.

The [3+2] cycloaddition of one equivalent of methyl azidoacetate to **1** in toluene at 90 °C afforded the triazole **12** as the only monoadduct. This process is regioselective with respect to the chain position (exclusive addition to the C-2/C-3 bond) and to the orientation of the N_3–R fragment within the heterocycle. In analogy to **7**–**11**, the chain position involved in the cycloaddition can be deduced from the ^{13}C NMR spectrum of **12**: for example, two signals for the two different cyano groups appear

at $\delta = 118$ and 104; the former can clearly be assigned to a CN group[27] that is not attached to a C–C triple bond, and the latter is typical for a CN group bound to a C≡C unit (see also NMR data of **1**–**11**). The proposed mode of azide addition for **12** (with N-1 attached to C-2 and N-3 to C-2) is strongly supported by the calculated polarizations (MP2 or AM1 Mulliken charges) of the C-2/C-3 bond in **1** and of the azide group in methyl azidoacetate, since C-2 is the more positively polarized C atom and N-1 the more negatively polarized N atom. The triazole **12** and the other newly synthesized cyanoeneynes **7**–**11** are nontrivial functionalized molecules, which are readily accessible in one step from dicyanopolyynes, such as **1** and **2**, and commercially available starting materials.

Conclusion

This work describes the one-step synthesis, isolation, and spectroscopic characterization of the dicyanopolyynes **1**–**6**. These rod-shaped molecules are short-chain model compounds for the hypothetical and presumably unstable linear sp-carbon allotrope carbyne sp-C_∞. The analysis of the spectroscopic behavior of **1**–**6** enables us to predict the electronic and NMR properties of carbyne. The CN end groups in **1**–**6** lead to pronounced polarization of the termini, especially of the triple bonds between C-2 and C-3. As a result [4+2] and [3+2] cycloadditions occur regioselectively at these positions. With the facile access to the stereochemically defined mono- and bisaddition products **7**–**12** in only one step, we have shown that dicyanopolyynes, which are themselves readily accessible in one step from graphite, can be useful as starting materials for the synthesis of interesting compound classes.

Experimental Section

General: ^{1}H NMR and ^{13}C NMR: Bruker AC250, Bruker ARX250, Bruker AMX400, Jeol JNM EX400, and Jeol JNM GX400; MS: Varian MAT711 (FD); IR: Bruker FT-IR IFS48 and Bruker FT-IR Vector 22; UV/Vis: Shimadzu UV 3102 PC; HPLC preparative: Shimadzu SIL 10A, SPD 10A, CBM 10A, LC 8A, FRC 10A (Grom-Sil 100 Si, NP1, 5 μ, 25 × 4.6 cm; Grom-Sil ODS 2, 5 μ, 25 × 2 cm); TLC (Machery-Nagel, Alugram® G/UV$_{254}$).

Reagents were prepared according to common procedures. Materials and solvents were obtained from commercial suppliers and were used without further purification. Products were isolated where possible by column or flash column chromatography (silica gel 60, particle size 0.04–0.063 nm, Merck).

Crystal data for 10: $M_r = 720.91$; triclinic; space group $P\bar{1}$; cell dimensions: $a = 9.140(2)$, $b = 10.118(2)$, $c = 11.882(2)$ Å, $\alpha = 67.72(2)$, $\beta = 78.36(2)$, $\gamma = 75.27(2)°$; $V = 983.3(3)$ Å^3; $\rho_{calc} = 1.217$ Mg m^{-3}; $Z = 1$; $F(000) = 382$; graphite monochromated Mo$_{K\alpha}$ radiation ($\lambda = 0.71073$ Å); $T = 173(2)$ K. Data were collected with a Nonius MACH3 diffractometer equipped with a rotating anode on a crystal with the dimensions $0.2 \times 0.3 \times 0.3$ mm. Data collecting range: $4.0 < 2\theta < 52.0°$. Of a total of 3989 collected reflections 3989 were unique and 2438 with $I > 2\sigma(I)$ were observed. The structure was solved by direct methods using SHELXS 86. 356 parameters were refined with all data by full-matrix least-squares on F^2 using SHELXL 93 (G. M. Sheldrick, Göttingen 1993). All non-hydrogen atoms were refined anisotropically. The hydrogen atoms were fixed in idealized positions using a riding model. Final R values: $R1 = 0.0774$ [$I > 2\sigma(I)$] and $wR2 = 0.2627$ (all data) with $R1 = \sum|F_o - F_c|/\sum F_o$ and $wR2 = \sum w|(F_o^2 - F_c^2)^2|/\sum w(F_o^2)^2)^{0.5}$; largest peak (0.456 e Å^{-3}) and hole (−0.484 e Å^{-3}).

Crystallographic data (excluding structure factors) for the structure reported in this paper have been deposited with the Cambridge Crystallographic Data Centre as supplementary publication no. CCDC-100173. Copies of the data can be obtained free of charge on application to The Director, CCDC, 12 Union Road, Cambridge CB2 1EZ, UK (Fax: Int. Code +(1223)336-033; e-mail: deposit@chemcrys.cam.ac.uk).

Synthesis of the dicyanopolyynes 1–6: Cyanogen was prepared according to literature[111] and condensed into an evacuated autoclave. The autoclave was then connected via a bubble counter to the gas inlet valve of a fullerene reactor.[1] The reactor was equipped with a graphite rod, and repeatedly evacuated and flushed with helium to 900 mbar. At the end of this procedure the reactor was filled with helium to 140–160 mbar, and the belljar was cooled with water. The reaction was started by applying a current of about 40–60 A, and opening the cyanogen valve. The gas stream was controlled to maintain an almost constant pressure in the reactor. After the reaction was finished, the reactor again was filled with helium and allowed to cool to room temperature. The mixture of the dicyanopolyacetylenes was removed from the belljar by extraction with toluene, and the soot removed from the solution by filtration. The polyyne solution was kept in the refrigerator. Yield: 7% with respect to graphite and 50% with respect to cyanogen.

Isolation of the dicyanopolyynes 1–6: The mixture of the dicyanopolyynes **1**–**6** was prepurified by flash column chromatography using toluene/hexane (80:20) as eluent. The solvent was evaporated at 30 °C under reduced pressure. The residue was dissolved in dry acetonitrile and the dicyanopolyacetylenes separated by preparative HPLC with a RP18-phase column using dry acetonitrile as eluent. With a flow of 20 mL min^{-1} it was possible to separate $C_{12}N_2$ (**3**), $C_{14}N_2$ (**4**), $C_{16}N_2$ (**5**), and $C_{18}N_2$ (**6**). C_8N_2 (**1**) and $C_{10}N_2$ (**2**) were obtained as a mixture and were separated in a second run with a flow of 5 mL min^{-1}. After separation toluene was added to the corresponding solutions and the acetonitrile was removed on a rotary evaporator. The resulting toluene solutions were stored in the refrigerator. Relative yields: C_8N_2 (**1**): 55%, $C_{10}N_2$ (**2**): 35%, and $C_{12}N_2$ (**3**): 7% (^{13}C NMR); $C_{14}N_2$ (**4**): 2%, $C_{16}N_2$ (**5**): 0.7%, and $C_{18}N_2$ (**6**): 0.3% (HPLC, UV det. at $\lambda = 280$ nm).

1,6-Dicyano-1,3,5-hexatriyne (1): ^{13}C NMR ($CDCl_3$, 25 °C): $\delta = 51.19$, 63.27, 65.64, 104.10 (*C*N); IR (NaCl): $\tilde{\nu} = 2247$ (C≡N), 2237 (C≡N), 2187 (C≡C) cm^{-1}; UV/Vis (acetonitrile): $\lambda_{max} = 232$, 222, 212, 203 nm; CV ($E_{1/2}$, 20 mV s^{-1}): −0.56 V; MS (70 eV, EI): $m/z = 124$ [M^+].

1,8-Dicyano-1,3,5,7-octatetrayne (2): ^{13}C NMR ($CDCl_3$, 25 °C): $\delta = 51.99$, 61.92, 64.56, 66.21, 104.28 (*C*N); IR (NaCl): $\tilde{\nu} = 2237$ (C≡N), 2186 (C≡C), 2120 (C≡C) cm^{-1}; UV/Vis (acetonitrile): $\lambda_{max} = 259$, 246, 235, 223 nm; CV ($E_{1/2}$, 20 mV s^{-1}): −0.55 V; MS (70 eV, EI): $m/z = 148$ [M^+].

1,10-Dicyano-1,3,5,7,9-decapentayne (3): ^{13}C NMR ($CDCl_3$, 25 °C): $\delta = 49.97$, 60.54, 62.54, 64.42, 65.94, 103.89 (*C*N); IR (NaCl): $\tilde{\nu} = 2237$ (C≡N), 2187 (C≡C), 2118 (C≡C) cm^{-1}; UV/Vis (acetonitrile): $\lambda_{max} = 282$, 267, 254, 242, 232 nm; CV ($E_{1/2}$, 20 mV s^{-1}): −0.40 V; MS (70 eV, EI): $m/z = 172$ [M^+].

1,12-Dicyano-1,3,5,7,11-dodecahexayne (4): ^{13}C NMR ($CDCl_3$, 25 °C): $\delta = 50.34$, 60.76, 62.55, 63.80, 65.38, 66.71, 104.49 (*C*N); IR (NaCl): $\tilde{\nu} = 2233$ (C≡N), 2170 (C≡C), 2154 (C≡C) cm^{-1}; UV/Vis (acetonitrile): $\lambda_{max} = 303$, 286, 271, 258, 246, 207 nm; MS (70 eV, EI): $m/z = 196$ [M^+].

1,14-Dicyano-1,3,5,7,9,11,13-tetradecaheptayne (5): IR (NaCl): $\tilde{\nu} = 2239$ (C≡N), 2172 (C≡C), 2128 (C≡C), 2092 (C≡C) cm^{-1}; UV/Vis (acetonitrile): $\lambda_{max} = 322$, 304, 287, 273, 260, 222 nm; MS (70 eV, EI): $m/z = 220$ [M^+].

1,16-Dicyano-1,3,5,7,9,11,13,15-hexadecaoctayne (6): IR (NaCl): $\tilde{\nu} = 2239$ (C≡N), 2172 (C≡C), 2126 (C≡C), 2092 (C≡C) cm^{-1}; UV/Vis (acetonitrile): $\lambda_{max} = 339$, 319, 301, 286, 271, 234 nm; MS (70 eV, EI): $m/z = 244$ [M^+].

2-Cyano-3-(4′-cyanobuta-1,3-diynyl)-5,6;7,8-dibenzo-1,4-dimethylbicyclo[2.2.2]oct-2-ene (7): 9,10-Dimethylanthracene (100 mg, 0.48 mmol) was added to a solution of triyne **1** (60 mg, 0.48 mmol) in 50 mL of toluene. This solution was stirred for 24 h at room temperature, and the product was

0947-6539/97/0307-1110 $ 17.50+.50/0 Chem. Eur. J. 1997, 3, No. 7

separated by flash column chromatography with toluene as eluent (yield: 54 mg, 39%, yellow powder). ^{1}H NMR (400 MHz, $CDCl_3$, 25 °C): δ = 2.28 (s, 3H, CH_3), 2.32 (s, 3H, CH_3), 7.14 (m, 4H, Ar-H), 7.34 (m, 4H, Ar-H); ^{13}C NMR (100.50 MHz, $CDCl_3$, 25 °C): δ = 13.93 (1C, CH_3), 14.02 (1C, CH_3), 50.68 (1C, bridgehead-C), 52.49 (1C, bridgehead-C), 61.28 (1C, C≡C),65.65 (1C, C≡C), 72.64 (1C, C≡C), 87.79 (1C, C≡C), 104.88 (1C, C≡N), 114.02 (1C, C≡N), 121.10 (2C, Ph-C), 121.20 (2C, Ph-C), 125.76 (2C, Ph-C), 125.91 (2C, Ph-C), 141.01 (1C, C=C), 145.00 (2C, Ph-C), 145.22 (2C, Ph-C), 148.99 (1C, C=C); MS (70 eV, EI): *m/z* (%): 330 (100) [M^+], 315 (80) [$M^+ - CH_3$], 206 (21) [DMA^+]; IR (KBr): $\tilde{\nu}$ = 3088 (Ar-H), 2977 (CH_3), 2925 (CH_3), 2849 (CH_3), 2235(C≡N), 2209 (C≡N), 2182 (C≡C), 1625 (C=C), 1453 (CH_3), 1386 (CH_3), 753 (Ar-H) cm^{-1}; UV/Vis (cyclohexane): λ_{max} (ε) = 365 (4500), 317 (4600), 292 nm (5500).

2-Cyano-3-(6′cyanohexa-1,3,5-triynyl)-5,6;7,8-dibenzo-1,4-dimethylbicyclo-[2.2.2]oct-2-ene (8) and 1,4-Di-(2-cyano-5,6;7,8-dibenzo-1,4-dimethylbicyclo-[2.2.2]oct-2-enyl)buta-1,3-diyne (11): Tetrayne **2** (87 mg, 0.58 mmol) and 9,10-dimethylanthracene (182 mg, 0.88 mmol) were dissolved in 50 mL of toluene and stirred for 3 h under reflux. The monoadduct **8** was separated from product **11** by column chromatography with toluene as eluent (yield: 21 mg, 10% **8**, yellow powder). ^{1}H NMR (400 MHz, $CDCl_3$, 25 °C): δ = 2.20 (s, 3H, CH_3), 2.26 (s, 3H, CH_3), 7.01 (m, 4H, Ar-H), 7.22 (m, 4H, Ar-H); ^{13}C NMR (100.50 MHz, $CDCl_3$, 25 °C): δ = 14.39 (1C, CH_3), 14.46 (1C, CH_3), 49.94 (1C, bridgehead-C), 52.01 (1C, C≡C), 52.12 (1C, bridgehead-C), 77.64 (1C, C≡C), 79,01 (1C, C≡C), 99.33 (1C, C≡C), 99.87 (1C, C≡C), 100.86 (1C, C≡C), 105.48 (1C, C≡N), 115.24 (1C, C≡N), 120,67 (2C, Ph-C), 120.72 (2C, Ph-C), 125.54 (4C, Ph-C), 133.73 (C=C), 145.79 (2C, Ph-C), 153.26 (1C, C=C); MS (70 eV, EI): *m/z* (%): 354 (20) [M^+], 339 (24) [$M^+ - CH_3$], 91 (25), 83 (100); IR (KBr): $\tilde{\nu}$ = 3068 (Ar-H), 2976 (CH_3), 2925 (CH_3), 2852 (CH_3), 2244 (C≡N), 2204 (C≡N), 2127 (C≡C), 1448 (CH_3), 1385 (CH_3), 736 (Ar-H) cm^{-1}; UV/Vis (cyclohexane): λ_{max} (ε) = 405 (4100), 379 (4400), 260 nm (5200).

The prepurified product **11** was dissolved in 1,1,2,2-tetrachlorethane and purified with preparative HPLC on a reversed phase column using acetonitrile as eluent with a flow of 10 mL min^{-1} (yield: 20 mg, 6% **11**, yellow powder). ^{1}H NMR (400 MHz, $CDCl_3$, 25 °C): δ = 2.23 (s, 6H, CH_3), 2.29 (s, 6H, CH_3), 7.09 (m, 8H, Ar-H), 7.31 (m, 8H, Ar-H); ^{13}C NMR (100.50 MHz, $CDCl_3$, 25 °C): δ = 14.06 (2C, CH_3), 14.21 (2C, CH_3), 50.07 (2C, bridgehead-C), 52.65 (2C, bridgehead-C), 80.65 (2C, C≡C), 89.88 (2C, C≡C), 72.64 (1C, C≡C), 114.80 (2C, C≡N), 120.79 (4C, Ph-C), 121.21 (4C, Ph-C), 125.54 (4C, Ph-C), 125.63 (4C, Ph-C), 135.83 (2C, C=C), 145.60 (4C, Ph-C), 145.73 (4C, Ph-C), 151.18 (2C, C=C); MS (70 eV, EI): *m/z* (%): 560 (38) [M^+] 545 (12) [$M^+ - CH_3$], 343 (51), 328 (20), 206 (100) [DMA^+], 191 (19) [$DMA^+ - CH_3$]; IR (KBr): $\tilde{\nu}$ = 3069 (Ar-H), 2977 (CH_3), 2924 (CH_3), 2852 (CH_3), 2208 (C≡N), 2127 (C≡C), 1448 (CH_3), 1386 (CH_3), 733 cm^{-1}(Ar-H); UV/Vis (acetonitrile): λ_{max} (ε) = 390 (11 300), 365 (10400), 262 nm (18900).

1-Cyano-2-(4′-cyanobuta-1,3-diynyl)-4,5-dimethyl-1,4-cyclohexadiene (9): 2,3-Dimethylbutadiene (89 mg, 1.08 mmol) was added to a solution of triyne **1** (134 mg, 1.08 mmol) in 50 mL of toluene. The mixture was stirred for 10 h at 60 °C. The product was purified over a silica gel column with toluene as eluent. Preparative HPLC was used for the separation using a silica gel column and cyclohexane/ethyl acetate (99:1) as eluent (yield: 48 mg, 22%, yellow-brown powder). ^{1}H NMR (400 MHz, $CDCl_3$, 25 °C): δ = 1.64 (s, 6H, CH_3), 2.88 (q, 4H, CH_2); ^{13}C NMR (100.50 MHz, $CDCl_3$, 25 °C): δ = 17.88 (1C, CH_3), 17.92 (1C, CH_3), 35.07 (1C, CH_2), 36.05 (1C, CH_2), 57.49 (1C, C≡C), 66.08 (1C, C≡C), 76.59 (1C, C≡C), 78.06 (1C, C≡C), 104.92 (1C, C≡N), 116.59 (1C, C≡N), 120.63 (1C, C=C), 121.03 (1C, C=C), 122.07 (1C, C=C), 130.02 (1C, C=C); MS (70 eV, EI): *m/z* (%): 206 (100) [M^+], 191 (85) [$M^+ - CH_3$], 164 (54), 57 (21), 43 (23); IR (KBr): $\tilde{\nu}$ = 2921 (CH_3), 2869 (CH_2), 2240(C≡N), 2205 (C≡N), 2104 (C≡C), 1597 (C=C), 889 cm^{-1} (CH_3); UV/Vis (cyclohexane): λ_{max} (ε) = 328 (10600), 307 (11100), 289 (6900), 273 nm (3000).

1,2-Di-(2-cyano-5,6;7,8-dibenzo-1,4-dimethylbicyclo[2.2.2]oct-2-enyl)ethyne (10): Triyne **1** (82 mg, 0.61 mmol) and 9,10-dimethylanthracene (271 mg, 1.32 mmol) were dissolved in 50 mL toluene and stirred for 3 h under reflux. The product was purified by flash column chromatography using toluene as eluent. For the recrystallization the residue was dissolved in cyclohexane under reflux and then allowed to cool to room temperature (yield: 138 mg, 23%, yellow crystals). ^{1}H NMR (400 MHz, $CDCl_3$, 25 °C): δ = 2.27 (s, 6H, CH_3), 2.32 (s, 6H, CH_3), 7.07 (m, 8H, Ar-H), 7.31 (m, 8H, Ar-H); ^{13}C NMR (100.50 MHz, $CDCl_3$, 25 °C): δ = 14.12 (2C, CH_3), 14.39 (2C, CH_3), 49.92 (2C, bridgehead-C), 50.09 (2C, bridgehead-C), 99.33 (2C, C≡C), 115.18 (1C, C≡N), 120.68 (4C, Ph-C), 120.79 (4C, Ph-C), 121.30 (4C, Ph-C), 125.49 (4C, Ph-C), 133.98 (2C, C=C), 145.75 (4C, Ph-C), 145.86 (4C, Ph-C), 152.02 (2C, C=C); MS (70 eV, EI): *m/z* (%): 536 (100) [M^+], 521 (21) [$M^+ - CH_3$], 319 (18), 304 (68), 206 (91), [DMA^+], 191 (30) [$DMA^+ - CH_3$], 91 (55), 28 (72); IR (KBr): $\tilde{\nu}$ = 3068 (Ar-H), 2977 (CH_3), 2943 (CH_3), 2881 (CH_3), 2201 (C≡N), 1601 (C=C), 1448 (CH_3), 1385 (CH_3), 736 cm^{-1} (Ar-H); UV/Vis (cyclohexane): λ_{max} (ε) = 379 (15500), 360 (10800), 299 (8800), 269 nm (7600).

5-Cyano-4-(4′-cyanobuta-1,3-diynyl)-1-methoxycarbonylmethyl-1,2,3-triazole (12): To a solution of triyne **1** (108 mg, 0.87 mmol) in 50 mL of toluene was added methyl azidoacetate (100 mg, 0.87 mmol). The solution was stirred at 90 °C overnight, and the product purified by column chromatography using a mixture of cyclohexane/ethyl acetate 3/1 to 2/1 as eluent (yield: 47 mg, 23%, white powder). ^{1}H NMR (400 MHz, $CDCl_3$, 25 °C): δ = 3.83 (s, 3H, CH_3), 5.28 (s, 2H, CH_2); ^{13}C NMR (100.50 MHz, $CDCl_3$, 25 °C): δ = 50.95 (1C, CH_3), 53.93 (1C, CH_2), 58.13 (1C, C≡C-CN), 65.31 (1C, C≡C), 65.71 (1C, C≡C), 79.22 (1C, C≡C), 104.62 (1C, C≡N), 106.18 (1C, C=C), 118.14(1C, C≡N), 133.67 (1C, C=C), 164.24 (1C, carbonyl-C); MS (70 eV, EI): *m/z* (%): 239 (8) [M^+], 211 (55) [$M^+ - N_2$], 152 (14), 139 (35), 124 (40), 59 (100) [$C_2H_3O_2^+$]; IR (KBr): $\tilde{\nu}$ = 2956 (CH_3), 2922 (CH_2), 2851 (OCH_3), 2239 (CN), 2219 (CN), 2138 (C≡C), 1757 (C=O), 1601 (C=C), 1541 (N=N), 1457 (CH_3), 1357 (CH_3), 1229 (C–O), 702 cm^{-1} (CH_2); UV/Vis (cyclohexane): λ_{max} (ε) = 322, 302, 285, 270 nm.

Acknowledgement: This work was supported by the Deutsche Forschungsgemeinschaft (DFG) and the Fond der Chemischen Industrie.

Received: January 23, 1997 [F 584]

[1] T. Grösser, A. Hirsch *Angew. Chem.* **1993**, *105*, 1390; *Angew. Chem. Int. Ed. Engl.* **1993**, *32*, 1340.
[2] For a recent review see: H. Hopf, B. Witulski in *Modern Acetylene Chemistry* (Eds.: P. J. Stang, F. Diederich), pp. 33, VCH Weinheim, **1995**.
[3] F. Diederich, Y. Rubin, *Angew. Chem.* **1992**, *104*, 1123; *Angew. Chem. Int. Ed. Engl.* **1992**, *31*, 1101.
[4] F. Bohlmann, *Chem. Ber.* **1953**, *86*, 63.
[5] F. Bohlmann, *Chem. Ber.* **1953**, *86*, 657.
[6] a) R. Eastmond, T. R. Johnson, D. R. M. Walton *Tetrahedron* **1972**, *28*, 4601; b) R. Eastmond, D. R. M. Walton *ibid.* **1972**, *28*, 4591; c) T. R. Johnson, D. R. M. Walton *ibid.* **1972**, *28*, 5221.
[7] Y. Rubin, S. S. Lin, C. B. Knobler, J. Anthony, A. M. Boldi, F. Diederich, *J. Am. Chem. Soc.* **1991**, *113*, 6943.
[8] T. Bartik, B. Bartik, M. Brady, R. Dembinski, J. A. Gladysz, *Angew. Chem.* **1996**, *108*, 467; *Angew. Chem. Int. Ed. Engl.* **1996**, *35*, 414.
[9] J. P. Hare, H. W. Kroto, *Acc. Chem. Res.* **1992**, *25*, 106.
[10] W. Krätschmer, L. D. Lamb, K. Fostiropoulos, D. R. Huffman, *Nature* **1990**, *347*, 354.
[11] D. J. Park, A. G. Stern, R. L. Willer, *Synth. Commun.* **1990**, *20* (18), 2901.
[12] R. J. Heath, Q. Zhang, S. C. O'Brien, R. F. Curl, H. W. Kroto, R. E. Smalley *J. Am. Chem. Soc.* **1987**, *109*, 359.
[13] A. A. Rohlfing, *J. Chem. Phys.* **1990**, *93*, 7851.
[14] M. Broyer, A. Goeres, M. Pellarin, E. Sedlmayer, J. L. Vialle, L. Wöste, *Chem. Phys. Lett.* **1992**, *198*, 128.
[15] A. Goeres, E. Sedlmayr, *Chem. Phys. Lett.* **1991**, *184*, 310.
[16] J. R. Chelikowsky, *Phys. Rev. Lett.* **1991**, *67*, 2970.
[17] C. Z. Wang, C. H. Xu, C. T. Chan, K. M. Ho, *J. Phys. Chem.* **1992**, *96*, 3563.
[18] J. R. Chelikowsky, *Phys. Rev. B* **1992**, *45*, 12062.
[19] R. Kerner, K. A. Penson, K. H. Bennemann, *Europhys. Lett.* **1992**, *19*, 363.
[20] G. von Helden, N. G. Gotts, M. T. Bowers, *Nature* **1993**, *363*, 60.
[21] M. T. Bowers, P. R. Kemper, G. von Helden, P. A. M. von Koppen, *Science* **1993**, *260*, 1446.
[22] G. von Helden, N. G. Gotts, M. T. Bowers, *J. Am. Chem. Soc.* **1993**, *115*, 4363.
[23] H. Schwarz, *Angew. Chem.* **1993**, *105*, 1475; *Angew. Chem. Int. Ed. Engl.* **1993**, *32*, 1412.

[24] a) G. Wegner, *Z. Naturforsch.* **1969**, B*24*, 824; b) G. Wegner, *Chimia* **1974**, *28*, 475; c) G. Wegner, *Makromol. Chem.* **1972**, *154*, 35; d) G. Wegner, *Makromol. Chem. Suppl.* **1984**, *6*, 347; e) G. Wegner, *Angew. Chem.* **1981**, *93*, 352; *Angew. Chem. Int. Ed. Engl.* **1981**, *20*, 361.
[25] R. J. Lagow, J. J. Kampa, H.-C. Wei, S. L. Battle, J. W. Genge, D. A. Laude, C. L. Harper, R. Bau, R. C. Stevens, J. F. Haw, E. Munson, *Science* **1995**, *267*, 362.
[26] The higher homologues **5** and **6** are too unstable in solutions concentrated enough for carrying out ^{13}C NMR spectroscopy.
[27] *SpecInfo 3.1*, Chemical Concepts, Boschstrasse 12, 69469 Weinheim, Germany, **1995**.
[28] ZINDO/S from *HyperChem 4.5* Hypercube, Inc. Waterloo, Ontario N2L 3X2, Canada, 1995.
[29] a) H. D. Försterling, H. Kuhn, *Moleküle und Molekülanhäufungen*, Springer, New York, 1983; b) H. A. Staab, *Einführung in die theoretische Organische Chemie*, VCH, 4th ed., Weinheim, 1975.
[30] G. N. Lewis, M. Calvin *Chem. Revs.* **1939**, *26*, 237.
[31] SPARTAN 4.0 Wavefunction, 18401 Von Karman, Suite 370, Irvine, California 92715, United States, **1995**.
[32] R. Hoffmann, *Angew. Chem.* **1987**, *99*, 871; *Angew. Chem. Int. Ed. Engl.* **1987**, *26*, 846.
[33] E. J. Ginsburg, C. B. Gorman, R. H. Grubbs in *Modern Acetylene Chemistry* (Eds.: P. J. Stang, F. Diederich), pp. 353, VCH Weinheim, **1995**.

0947-6539/97/0307-1112 $ 17.50+.50/0